

See discussions, stats, and author profiles for this publication at: <https://www.researchgate.net/publication/202993345>

# Electron Transfer Kinetics of Cytochrome C in the Submillisecond Time Regime Using Time-Resolved Surface-Enhanced Infrared Absorption Spectroscopy

ARTICLE *in* THE JOURNAL OF PHYSICAL CHEMISTRY C · FEBRUARY 2009

Impact Factor: 4.77 · DOI: 10.1021/jp8071052

---

CITATIONS

16

---

READS

17

6 AUTHORS, INCLUDING:



Denise Schach

University of Chicago

18 PUBLICATIONS 109 CITATIONS

[SEE PROFILE](#)



Renate L. C. Naumann

AIT Austrian Institute of Technology

91 PUBLICATIONS 2,857 CITATIONS

[SEE PROFILE](#)

# A Two-Layer Gold Surface with Improved Surface Enhancement for Spectro-Electrochemistry Using Surface-Enhanced Infrared Absorption Spectroscopy

C. NOWAK, C. LUENING, W. KNOLL, and R. L. C. NAUMANN\*

Max Planck Institute for Polymer Research, Ackermannweg 10, 55128 Mainz, Germany (C.N., C.L., R.L.C.N.); and Austrian Research Centers GmbH, Tech Gate Vienna, Donau-City Str. 1, 1220 Vienna, Austria (W.K.)

A two-layer gold surface is developed for use with surface-enhanced infrared absorption spectroscopy (SEIRAS) consisting of a conducting underlayer onto which Au nanoparticles (AuNPs) are grown by self-catalyzed electroless deposition. AuNPs are grown on protruding substructures of the 25 nm thin underlayer. The enhancement factor of the two-layer gold surface is controlled by the growth conditions. Cytochrome c adsorbed to a self-assembled monolayer of mercaptoethanol is used as a reference system. Under optimum conditions the absorbance of the amide I band is increased by a factor of 5 versus the classical SEIRAS surface. Reversible reduction/oxidation of cytochrome c on the two-layer gold surface is shown to take place by cyclic voltammetry.

Index Headings: Surface-enhanced infrared absorption spectroscopy; SEIRAS; Cytochrome c; Spectro-electrochemistry; Gold nanoparticles.

## INTRODUCTION

One of the most powerful methods for the identification of small amounts of molecules and the molecular structure of adsorbed molecules is surface-enhanced infrared absorption spectroscopy (SEIRAS).<sup>1–3</sup> Like its counterpart, surface-enhanced Raman scattering (SERS),<sup>4</sup> SEIRAS relies on the morphology of the metal surface.<sup>2</sup> Thin metallic films consisting of metal islands<sup>5</sup> as well as monolayers of nanoparticles (NPs)<sup>1,6</sup> are good candidates. The surface enhancement is considered in terms of local enhancements of the electromagnetic field induced by local structures as well as charge transfer effects in chemical structures. Local field enhancement preferably occurs in the narrow gap between single islands or NPs smaller in size than the wavelength of light, which are kept at distances wide enough not to touch each other. SEIRAS has been applied on colloidal gold films assembled on attenuated total reflection (ATR) crystals for *in situ* monitoring the adsorption and chemical reaction of monomolecular layers.<sup>5,7–9</sup> In combination with electrochemical excitation, redox changes of the adsorbed layers could also be monitored in the time-resolved mode.<sup>10</sup>

Layers of islands can be prepared by electrothermal evaporation<sup>5</sup> or sputtering or by chemical (electroless) deposition techniques.<sup>11</sup> This technique was recently improved by using a two-step procedure to tailor the size and distance of metal colloid monolayers.<sup>1</sup> A sub-monolayer of AuNPs was assembled in a first step on a Si crystal. In a second step these AuNPs were grown to the desired size and distance by self-catalyzed electroless deposition. The enhancement effect could thus be varied systematically.<sup>9</sup> Electrochemical applications,

however, require a different design, with layers of sufficient conductivity. SEIRA surfaces for such purposes were prepared by assembling nanoparticles (NPs) of random distribution by the electroless deposition technique.<sup>11</sup> This technique, however, provides no effective control over the enhancement effect. Moreover, the adhesion of the NPs on the ATR crystal is often insufficient for extensive studies.

To overcome these drawbacks and at the same time obtain a more robust procedure to prepare SEIRAS surfaces applicable for spectro-electrochemistry, we introduced a different strategy. We began with a 25 nm thin Au underlayer evaporated on the Si crystal. This thickness provides the limiting condition to achieve a conducting layer of evaporated Au, although a closed film is not quite formed. This condition may not hold for other materials such as Si, where closed films are already obtained at much lower thicknesses. However, protruding structures on the 25 nm thick Au surface can be used effectively as seed crystals. AuNPs will grow predominantly on these sites rather than filling the gaps in the loose underlayer. The size of these NPs and at the same time, the enhancement factor, can be controlled by systematically varying the growth conditions as in previous studies.<sup>9</sup> A SEIRAS surface with a better enhancement factor can thus be obtained, which is also more reliable in terms of adhesion, conductivity, and stability over time. This was quantitatively investigated, using cytochrome c (cc) as a well-studied reference system.<sup>8,12–14</sup>

## MATERIALS AND METHODS

Hydroxylamine hydrochloride 99% ( $\text{NH}_2\text{OH HCl}$ ), gold(III) chloride hydrate 99.999% ( $\text{AuCl}_3 \cdot \text{H}_2\text{O}$ ), potassium chloride, potassium dihydrogenphosphate, and cytochrome c from bovine heart were purchased from Sigma-Aldrich. 2-Mercaptoethanol 99% extra pure was supplied by Acros. Sodium perchlorate was purchased from Fluka Biochemika, Buchs, Switzerland.

**Preparation of the Two-Layer Gold Film on the Flat Surface of the Silicon Crystal.** The two-layer gold surface is depicted schematically in Fig. 1. The surface of the silicon ATR crystal was polished prior to use with a polishing machine (Buehler PHOENIX 4000) using the polishing cloth TexMet P, VerduTex, and MicroCloth and MetaDi Supreme and polycrystalline diamond suspension, grain size 9  $\mu\text{m}$ , 3  $\mu\text{m}$ , and 1  $\mu\text{m}$ , in that order. The polished trapezoid crystal was ultrasonically cleaned with ethanol for 15 min. Then a thin (25 nm) gold film was deposited by electrothermal evaporation onto the flat surface of the ATR crystal using an evaporation machine (Edwards FL 400). Finally the crystal with the gold film was thoroughly rinsed with ethanol and dried with nitrogen. The gold film had a roughness of  $R_q = 2 \text{ nm}$ ,

Received 10 December 2008; accepted 22 June 2009.

\* Author to whom correspondence should be sent. E-mail: naumannr@mpip-mainz.mpg.de.

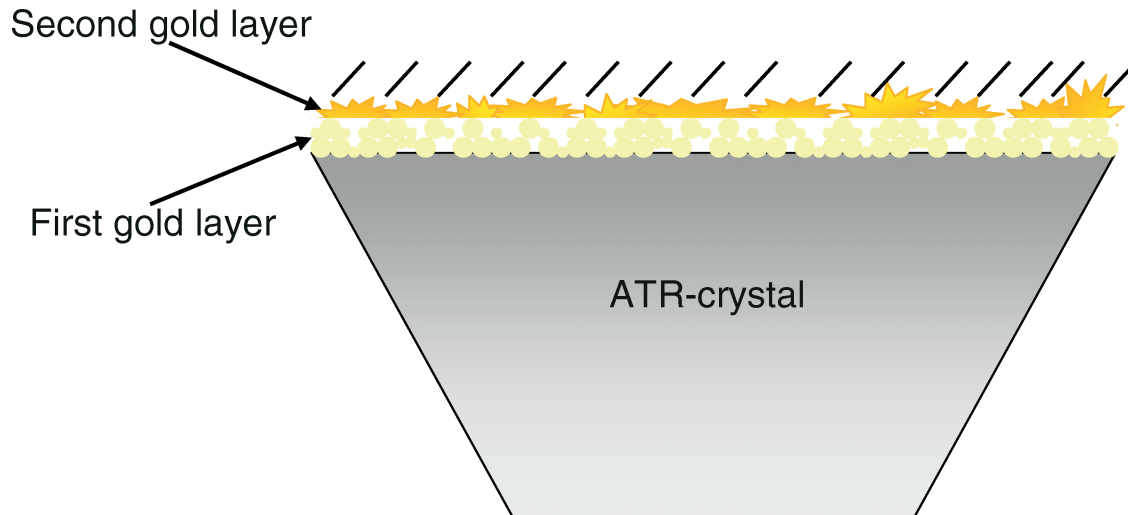


FIG. 1. Schematics of the trapezoidal silicon ATR crystal covered by the two-layer gold system. First layer: thermally evaporated gold layer (25 nm thickness). Second layer: chemically grown AuNPs from  $\text{AuCl}_3/\text{NH}_2\text{OH}$  growth solution. The two-layer gold system on the ATR crystal serves as the working electrode, at the same time providing a roughened surface required for the surface enhancement.

considering the resolution of the AFM in the lateral direction  $>10$  nm.

In order to grow NPs on the gold film, the crystal was immersed into 50 mL of an aqueous solution of hydroxylamine hydrochloride ( $\text{NH}_2\text{OH HCl}$ ) (0.4 mM) to which 500  $\mu\text{L}$  of an aqueous solution of gold (III) chloride hydrate (0.3 mM) was added. After 2 min, the same amount of  $\text{AuCl}_3$  solution was added. This process was repeated  $n$  times, where  $n$  determines the overall growth time. The process was terminated by removing the samples from the growth solution, rinsing them with water, and gently drying them in a stream of nitrogen.

These samples with the two-layer gold surface were immersed for 15 min into an aqueous solution of 2-

mercaptoethanol (ME) (1 mM) to form a self-assembled monolayer. After that the samples were rinsed with water and subsequently immersed in a PBS solution (20 mM  $\text{K}_2\text{HPO}_4/10$  mM  $\text{NaClO}_4/\text{pH } 7$ ).  $\text{NaClO}_4$  was used instead of  $\text{NaCl}$  or  $\text{KCl}$  in order to avoid the anodic dissolution of Au during cyclic voltammetry. After taking a reference spectrum of the gold-covered ATR crystal in buffer solution, cyt c (cc) was adsorbed from a solution of cc (0.35 mM) in the same buffer.

**Surface-Enhanced Infrared Absorption Spectroscopy.** The spectro-electrochemical cell is depicted in Fig. 2. A fluid cell with a lid, made from Teflon, was mounted on top of a trapezoid silicon ATR crystal required for a single reflection in the ATR mode. With the Si crystal covered with the two-layer

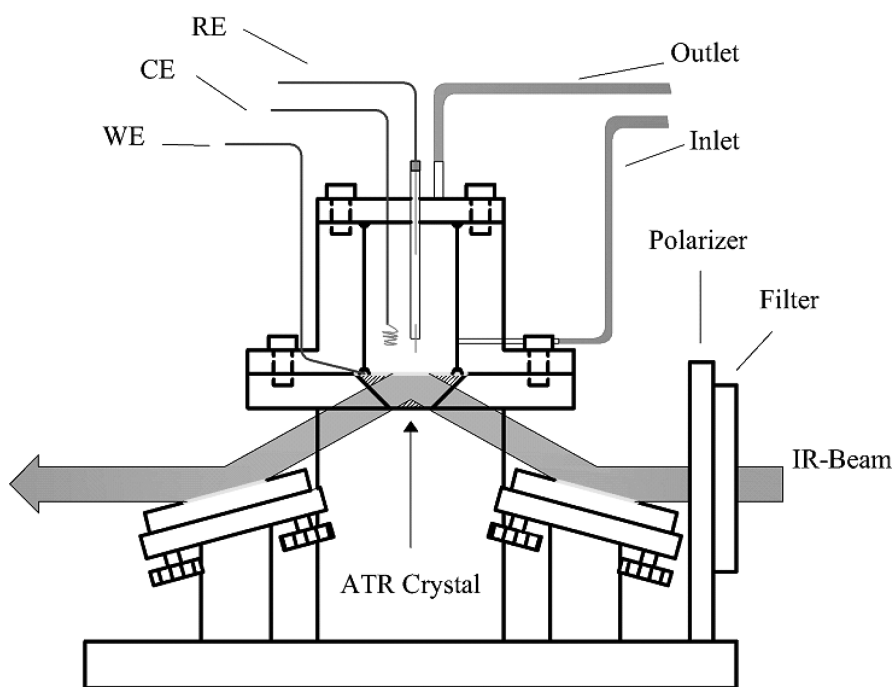


FIG. 2. The ATR-FT-IR spectro-electrochemical cell. The fluid cell provided with reference and counter electrodes is mounted on top of a trapezoidal silicon ATR crystal for use of the ATR mode. The gold layer on the ATR crystal serves as the working electrode.

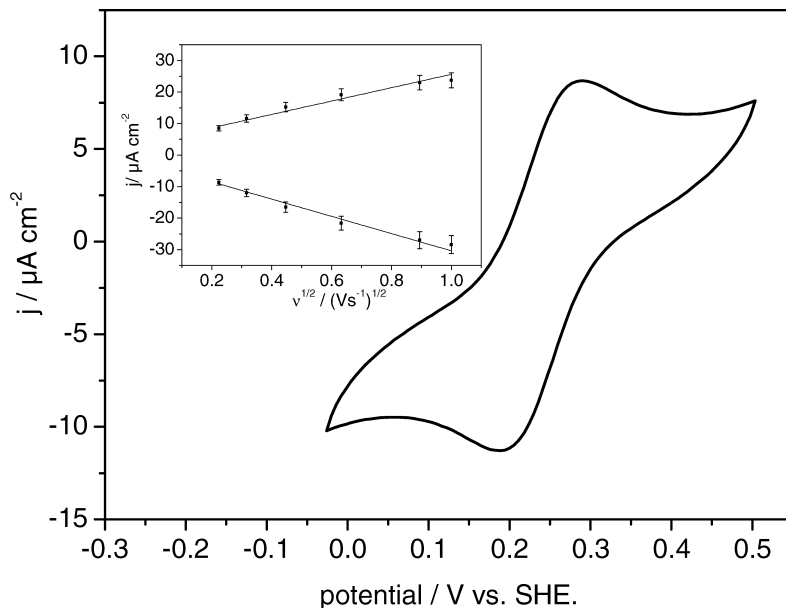


FIG. 3. Cyclovoltammogram of cc absorbed to the mercaptoethanol-modified two-layer gold surface taken at a scan rate of 50 mV/s with a cathodic peak at 274 mV and an anodic peak at 203 mV versus SHE. The peak separation is 71 mV. (Inset) Peak height of the cathodic peak and anodic peak versus the square root of scan rate.

gold film, the setup operates in the so-called ATR/Kretschmann configuration.<sup>2,15</sup> The IR beam of the Fourier transform infrared (FT-IR) spectrometer (VERTEX 70 FTIR spectrometer, from Bruker, Karlsruhe) was coupled into the prism at an angle of incidence  $\Theta = 60^\circ$ . The total reflected beam IR intensity was measured with a photovoltaic mercury cadmium telluride (MCT) detector. Spectra were recorded with  $4 \text{ cm}^{-1}$  spectral resolution. The mirror velocity was 120 kHz, the phase resolution was  $128 \text{ cm}^{-1}$ , and 5555 scans were taken for one spectrum during a measurement period of 10 min.

Spectra were analyzed by the software package OPUS 6 (Bruker, Karlsruhe).

**Electrochemical Measurements.** Electrochemical measurements were performed using an Autolab instrument (PGSTAT302) equipped with an ECD-module amplifier for low currents, an ADC750 module for rapid scan measurements, and a SCAN-GEN module for analog potential scanning (Eco Chemie, B.V., Utrecht, Netherlands). Measurements were done in a buffer solution containing 20 mM  $\text{K}_2\text{HPO}_4$ , 10 mM  $\text{NaClO}_4$ , pH 7, and all electrochemical measurements were taken in a three-electrode configuration with the gold film as the working electrode, an  $\text{Ag}/\text{AgCl}, \text{KCl}_{\text{sat}}$  reference, and a platinum wire as the counter electrode. All electrode potentials are quoted versus standard hydrogen electrode (SHE).

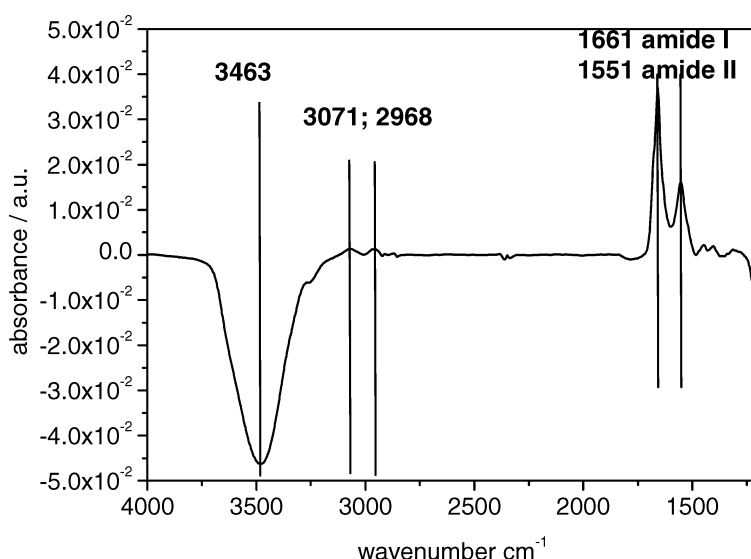


FIG. 4. ATR-FT-IR difference spectra after the immobilization of the cc on the ME-modified two-layer gold surface in the frequency range  $4000\text{--}1200 \text{ cm}^{-1}$ . The reference is the spectrum of the ME-modified gold electrode before the absorption of cc. Band assignment:  $3463 \text{ cm}^{-1}$ : OH stretching mode;  $3071 \text{ cm}^{-1}$ : protonated  $\text{NH}_2$  band of an amino acid;  $2968 \text{ cm}^{-1}$ : methyl mode;  $1661 \text{ cm}^{-1}$ : amide I;  $1551 \text{ cm}^{-1}$ : amide II.

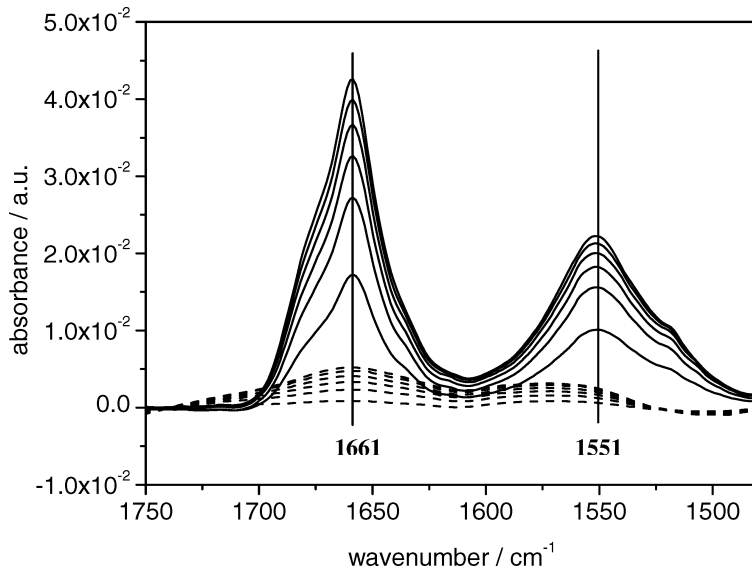


FIG. 5. ATR-FT-IR difference spectra of the amide I and II region of cc recorded as a function of time of cc absorption on the two-layer gold surface (solid lines) compared to a gold layer prepared according to the classical electroless deposition (broken lines). Spectra are taken every 10 min. The reference is the spectrum of the ME-modified electrode before the absorption of cc.

## RESULTS AND DISCUSSION

The two-layer Au film was optimized stepwise starting with the gold underlayer. Criteria of the optimization, however, could be applied only after the formation of the complete two-layer surface including cc absorption. In order to investigate the gold underlayer with respect to its electrochemical properties, for example, cc had to be adsorbed to the optimized two-layer surface after modifying it with a self-assembled monolayer of mercaptoethanol (ME). The optimization of the two intermediate steps will be described further below. Figure 3 shows the cyclic voltammogram of cc adsorbed on the two-layer gold surface. A gold underlayer of 25 nm thickness was found to be sufficient to provide a conducting film. Thinner underlayers

resulted in increasingly noisy signals (not shown). Cc was found to be electroactive, showing cathodic and anodic peaks at 274 and 203 mV and a standard redox potential of 238 mV, in agreement with literature values.<sup>16</sup> The peak separation of 71 mV indicated a diffusion-controlled process. This was also in agreement with the dependence of the peak height from the square root of the scan rate shown in the inset of Fig. 3. The peak width of 119 mV, however, is compatible with an adsorbed species at equilibrium with cc in solution (the theoretical peak width for a 1e reversible electron transfer (eT) of an adsorbed species is 90 mV).<sup>17</sup>

These monolayers of cc were also investigated with respect to their spectroscopic properties. SEIRA difference spectra were taken in the ATR configuration with the ME-modified

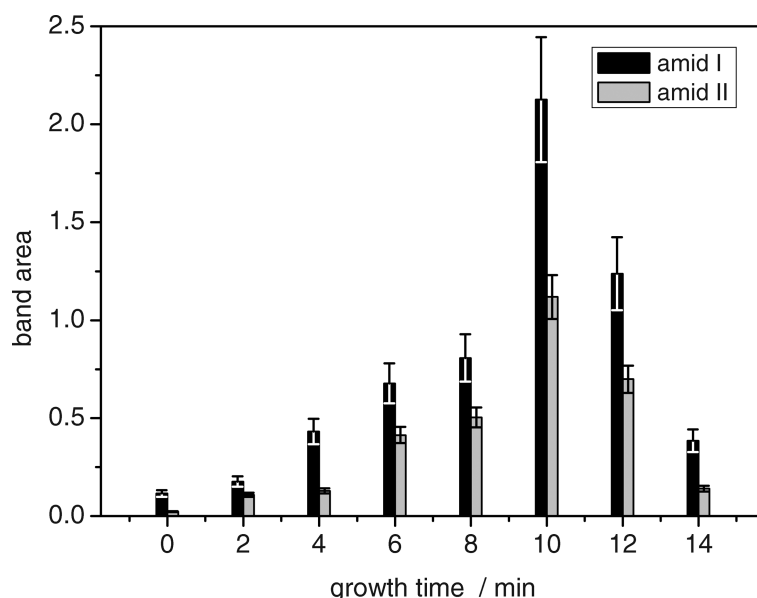


FIG. 6. The band area (absorbance times the range of wavelengths covered by the band) of amide I and II bands as a function of growth time of the second gold layer. The optimal growth time amounts to 10 min yielding the maximum enhancement effect.

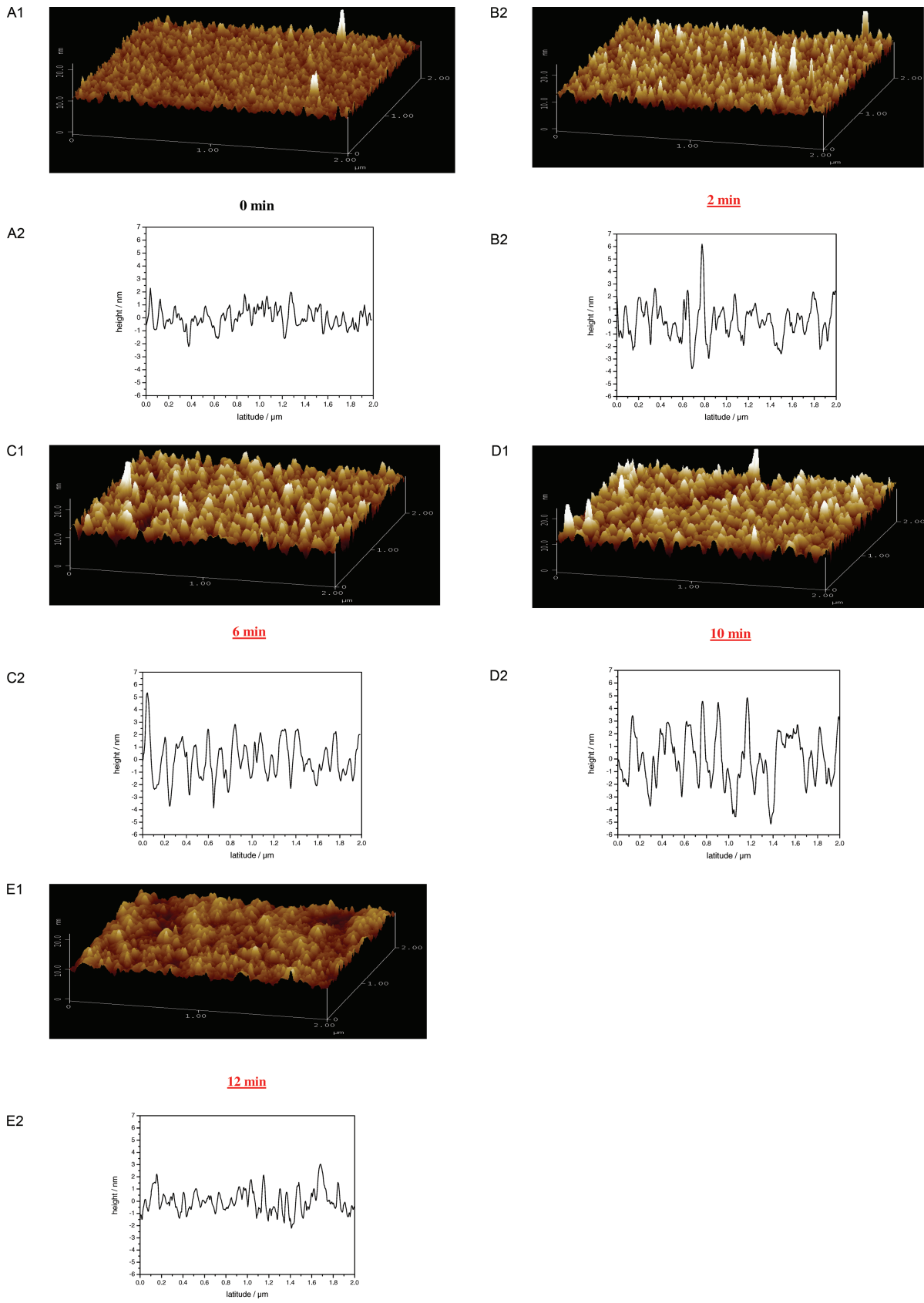


FIG. 7. AFM images of Au films obtained with different growth times (0, 2, 6, 10, and 12 min as indicated on the line scans). The AFM measurements were performed with a scanning probe microscope “Dimension 3100” from Veeco, NY. Measurements were carried out in the tapping mode with a silicon nitride cantilever in a triangular shape.

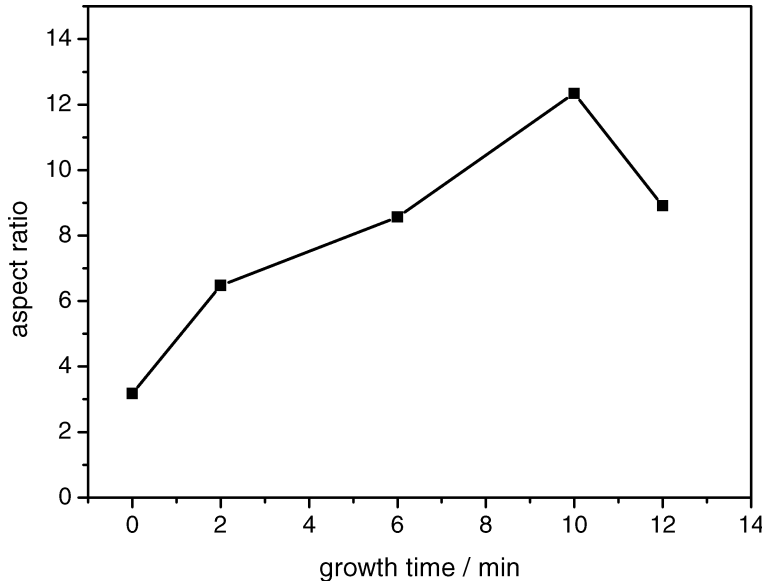


FIG. 8. Aspect ratio obtained from AFM images of NPs grown on protruding structures of evaporated gold as a function of growth time. The maximum correlates with the optimum of the enhancement effect illustrated in Fig. 6.

gold electrode as the reference. The absorbance  $A$  was calculated according to

$$A = -\log\left(\frac{I}{I_0}\right) \quad (1)$$

where  $I$  and  $I_0$  are the intensities of the sample and the reference, respectively.

Figure 4 shows the difference spectrum characterized by a strong negative band at  $3463\text{ cm}^{-1}$ , and two strong positive bands at  $1661\text{ cm}^{-1}$  and  $1551\text{ cm}^{-1}$ . The positive bands were assigned previously to the amide I ( $\text{C}=\text{O}$  stretching) and amide II ( $\text{NH}$  in-plane bending) vibrations of the protein backbone, respectively.<sup>7</sup> The negative band indicates the  $\text{O}-\text{H}$  stretching vibration of displaced water molecules. The band positions correspond to those reported in previous studies of cc in a similar architecture on a gold surface obtained by electroless deposition.<sup>8</sup> The amplitude of the bands in Fig. 6, however, is higher by a factor of 5 compared to the previous investigation (Ref. 8). Both are in good agreement with the spectrum of cc in solution.<sup>18</sup>

The SEIRA spectra thus obtained were used to investigate the time dependence of cc absorption. Figure 5 shows the amide I and II bands on the two-layer gold surface after different immersion times in the cc solution. A layer of AuNPs prepared by the classical chemical (electroless) deposition was used as a reference.<sup>11</sup> Adsorption was completed after 60 min in both cases. The bands on the two-layer gold surface, however, were enhanced by a factor of 10 as compared to the electroless deposition method. Comparison with the evaporated Au layer was not possible since SEIRA spectra of cc were not obtained on this surface. The enhancement factor of cc molecules adsorbed on the new surface as compared those in solution was calculated according to the procedure introduced by Osawa.<sup>2,12</sup> A value of 127.8 was found, 5.8 times the value of 22 found for the classical gold surface obtained by electroless deposition (see Ref. 19).

These experiments were done on the two-layer surface optimized with respect to the growth time. The optimization of

the growth time proper was done by varying the immersion time of the gold underlayer in the  $\text{AuCl}_3/\text{NH}_2\text{OH}$  growing solution. SEIRA spectra were taken after adsorption of cc under saturation conditions as described in the previous section. The result is illustrated in Fig. 6. Peak areas of the amide I and II bands are plotted as a function of growth time. The data are mean values of three repetitive measurements. As deduced from this result, the enhancement effect could be varied systematically, reaching the optimum at 10 min growth time, the condition used for all further measurements.

For the interpretation of these results, AFM images were taken starting from the evaporated underlayer and then following the growth of NPs as a function of time (Fig. 7). Although the NPs are randomly distributed in shape, they appear to grow systematically in size. This was deduced particularly from the evolution of the depth profile, also shown in the line scans of Fig. 7. NPs grow mainly with respect to the width rather than the height, until the height decreases after the percolation limit was reached at  $>10$  min growth time. This was analyzed by plotting the aspect ratio of width versus height versus growth time (Fig. 8). The maximum aspect ratio of 12.3 was reached at 10 min, which corresponds to the optimum of the enhancement effect. The aspect ratio was also one of the significant parameters in current theories of the surface enhancement. Particles with a high aspect ratio are considered more effective than particles with a low aspect ratio.<sup>3</sup>

In this context it was also interesting to inspect the difference between the two-layer surface and a layer formed on a seed layer of NPs (Ref. 1) as revealed by AFM, particularly concerning the line scan. The thickness of the two-layer surface was largely determined by the evaporated Au ( $\sim 25\text{ nm}$ ), while the NPs formed on protruding structures made up for an additional  $\sim 0.2\text{ nm}$  only. By contrast, the gold film formed on a seed layer of NPs had a similar overall thickness ( $\sim 25\text{ nm}$ ), which, however, was determined largely by the height of the NPs. The peak to valley height was about 22 nm (estimated from the line scans in Ref. 1) resulting in a considerable roughness, as compared to the two-layer surface, which had a

peak to valley height of 1.6 nm. A high roughness does not allow well-ordered monolayers of proteins or other compounds often required for spectro-electrochemistry. The diameter of the NPs grew with time in both cases, however, in a different fashion. The NPs described in Ref. 1 appeared to grow in two directions, increasing both in height and width, whereas the NPs of the two-layer surface seemed to grow mainly with respect to the width. As a result, the aspect ratio of NPs of Ref. 1 did not exceed 1.7, as estimated from the line scans of the AFM pictures, whereas the aspect ratio of the two-layer surface increased up to a maximum of 12.3 at 10 min growth time (Fig. 8). From this the two-layer surface could be expected to be superior. Unfortunately, a comparison with the layer formed on a seed layer of NPs could not be done experimentally because of difficulties we encountered in the preparation.

## CONCLUSION

Theory predicts that surface enhancement is obtained on surfaces with single islands of nm size.<sup>1,2</sup> Growth of NPs *in situ* has been shown before to yield surfaces with a controllable enhancement factor. This concept had been successfully applied to preformed NPs immobilized particularly on non-conducting surfaces.<sup>1,9</sup> A similar concept seems to work for thin conducting underlayers, whose protruding substructures are used as seed crystals rather than immobilized small NPs. The aspect ratio of the NPs thus obtained seems to be larger than the one obtained for NPs growing in both directions. The effect of islands percolating to larger structures can be observed in the AFM pictures of surfaces with growth times of more than 10 min. The optimum is achieved when AuNPs are grown to around 60 nm size. Under these conditions, the enhancement factor is appreciably improved over that of the classical chemical (electroless) deposition technology. The preparation

of the newly developed two-layer surface was greatly facilitated, while the thickness can be controlled very precisely. Moreover, the stability of the surfaces is much improved so as to allow long-term measurement of protein monolayers. This was demonstrated in Ref. 19 showing time-resolved spectro-electrochemical investigations of cc using SEIRAS.

1. S. J. Huo, Q. X. Li, Y. G. Yan, Y. Chen, W. B. Cai, Q. J. Xu, and M. Osawa, *J. Phys. Chem. B* **109**, 15985 (2005).
2. M. Osawa, "Surface-Enhanced Vibrational Spectroscopy", in *Handbook of Vibrational Spectroscopy* (John Wiley and Sons, Chichester, 2001).
3. M. Osawa, K. Ataka, K. Yoshii, and Y. Nishikawa, *Appl. Spectrosc.* **47**, 1497 (1993).
4. A. Otto, I. Mrozek, H. Grabhorn, and W. Akemann, *J. Phys. Condens. Mat.* **4**, 1143 (1992).
5. A. Pucci, *Phys. Stat. Solidi B* **242**, 2704 (2005).
6. Y. Nishikawa, T. Nagasawa, K. Fujiwara, and M. Osawa, *Vib. Spectrosc.* **6**, 43 (1993).
7. K. Ataka, F. Giess, W. Knoll, R. Naumann, S. Haber-Pohlmeier, B. Richter, and J. Heberle, *J. Am. Chem. Soc.* **126**, 16199 (2004).
8. K. Ataka and J. Heberle, *J. Am. Chem. Soc.* **126**, 9445 (2004).
9. D. Enders, T. Nagao, A. Pucci, and T. Nakayama, *Surf. Sci.* **600**, L71 (2006).
10. K. Ataka, Y. Hara, and M. Osawa, *J. Electroanal. Chem.* **473**, 34 (1999).
11. H. Miyake, S. Ye, and M. Osawa, *Electrochim. Commun.* **4**, 973 (2002).
12. K. Ataka and J. Heberle, *Biopolymers* **82**, 415 (2006).
13. K. Ataka and J. Heberle, *Anal. Bioanal. Chem.* **388**, 47 (2007).
14. X. U. Jiang, K. Ataka, and J. Heberle, *J. Phys. Chem. C* **112**, 813 (2008).
15. R. Aroca, *Surface-Enhanced Vibrational Spectroscopy* (Wiley and Sons, Chichester, 2006).
16. A. S. Haas, D. L. Pilloud, K. S. Reddy, G. T. Babcock, C. C. Moser, J. K. Blasie, and P. L. Dutton, *J. Phys. Chem. B* **105**, 11351 (2001).
17. A. J. Bard and L. R. Faulkner, *Electrochemical Methods and Applications* (John Wiley and Sons, New York, 2001).
18. A. Dong, P. Huang, and W. S. Caughey, *Biochemistry-U.S* **31**, 182 (1992).
19. C. Nowak, C. Luening, D. Schach, D. Bauricht, W. Knoll, and R. L. C. Naumann, *J. Phys. Chem. C* **113**, 2256 (2009).